N84 27289

ALTIMETER HEIGHT MEASUREMENT ERRORS INTRODUCED BY THE PRESENCE OF VARIABLE CLOUD AND RAIN ATTENUATION

Francis M. Monaldo and Julius Goldhirsh
The Johns Hopkins University/Applied Physics Laboratory
Johns Hopkins Road, Laurel, Maryland 20707

Edward J. Walsh
NASA/Goddard Space Flight Center
Wallops Flight Facility
Wallops Island, Virginia 23337

ABSTRACT

It has recently been recognized that spatially inhomogeneous clouds and rain can substantially affect the height precision obtainable from a spaceborne radar altimeter system (Walsh, et al., 1983). Through computer simulation, it has been found that typical levels of cloud and rain intensities and associated spatial variabilities may degrade altimeter precision at 13.5 GHz and, in particular, cause severe degradation at 35 GHz. This degradation in precision is a result of radar signature distortion caused by variable attenuation over the beam limited altimeter footprint. Because attenuation effects increase with frequency, imprecision caused by them will significantly impact on the frequency selection of future altimeters.

In this paper we examine the degradation of altimeter precision introduced by idealized cloud and rain configurations as well as for a realistic rain configuration as measured with a ground based radar.

1. INTRODUCTION

As the requirements for precision in geodetic surveys grow more stringent and as physical oceanographers begin to exploit altimeter data to study ocean-wide circulation dynamics, the precision demands on height measurements by future radar altimeters become more severe. Hence, error sources that could previously be legitimately ignored must now be considered. The precision degradation caused by spatially variable cloud and rain attenuation patterns is one such error source.

When the narrow radar pulse transmitted from the altimeter reflects from the ocean surface it is significantly spread by the ocean surface roughness. This pulse broadening, while valuable in that it provides an estimate of ocean surface wave height, degrades the ability of the altimeter to measure the range between the satellite and the surface. To reconstruct the position of the leading edge of the pulse, the entire pulse waveform shape is processed in a tracking algorithm. Distortion of this waveform shape will necessarily degrade the precision with which the track point can be determined.

The beam-limited surface footprints of spaceborne radar altim-

eters of the Seasat class are on the order of 20 km. If the rain and cloud attenuation is uniform over an altimeter footprint, the total return signal power is reduced, the waveform shape remains unchanged and the altimeter tracking algorithm height estimate is unaffected. In this paper we focus on the situation where altimeter precision is degraded because attenuation levels within the footprint are laterally inhomogeneous, distorting the return waveform shape.

2. RAIN CELL AND CLOUD ATTENUATION LEVELS AND SCALE SIZES

Cloud liquid water content and rain intensity vary considerably both spatially and temporally. As such, these quantities should be dealt with statistically. This section is designed to give the reader a general appreciation of these quantities. Later we will consider the computer simulation of the passage of an altimeter over various plausible, idealized cloud and rain attenuation patterns as well as the passage of such an altimeter over actual, measured rain cells to determine the effect of these on altimeter measurement of range to the sea surface.

2.1 Clouds

Cloud liquid water content, upon which attenuation depends, is highly variable. Liquid water content may fluctuate between a small fraction to several gm/m^3 over a cloud width of 1 to 2 km (Ackerman, 1959). Ackerman (1967) has also measured liquid water contents ranging from 0.5 to 2.5 gm/m^3 over distances exceeding 9 km. To the authors' knowledge there are no statistics available relating cloud size directly to liquid water content levels. However, Lopez (1977) and Kuettner (1971) have determined typical scale dimensions for the cumulus clouds and cloud streets based on either optical or refractive measurements to be on the order of several kilometers.

Interpolating the results of Gunn and East (1954), the attenuation coefficient, normalized to cloud liquid water content, is approximately 0.17 $(dB/km)/(gm/m^3)$ at 13.5 GHz and 1.1 $(dB/km)/(gm/m^3)$ at 35 GHz. Cole (1961) has provided average liquid water contents for various common cloud types.

Table 1 summarizes and combines these results by estimating the average two-way attenuation through a 1 km thick cloud for four common cloud types at both 13.5 and 35 GHz. Note that the total attenuation may vary between 0.034 and .85 dB at 13.5 GHz and 0.22 and 5.5 dB at 35 GHz.

2.2 Rain

Assuming a Marshall-Palmer (1948) drop size distribution, the attenuation coefficient at 13.5 GHz is 0.06 dB/km at the small rain rate of 2 mm/hr, 0.4 dB/km at the moderate rain rate of 10 mm/hr, and 0.9 dB/km at the large rain rate of 20 mm/hr. At 35 GHz, the attenuation coefficients are 0.5, 2.4, and 5.0 dB/km for the rain rates, 2, 10, and 20 mm/hr, respectively (Goldhirsh and Rowland, 1982). Table 2 summarizes the results by providing the two-way attenuation at 13.5 and 35 GHz, at various rain rates for both a

Table 1 Cloud Attenuation Levels

Frequency (GHz)	Normalized Attenuation Coefficient (dB/km)/(gm/m^3)	Cloud Type	Liquid Water Content (gm/m^3)	Total, Two-Way Attenuation Thru a 1 km Thick (dB)
13.5	0.17	Stratiform	0.1-0.2	0.034-0.068
		Cumulus Humilis	1.0	0.34
		Cumulus Congestus	2.0	0.68
		Cumulonimbus	2.5	0.85
35	1.1	Stratiform	0.1-0.2	0.22-0.44
		Cumulus Humilus	1.0	2.2
		Cumulus Congestus	2.0	4.4
		Cumulonimbus	2.5	5.5

Table 2 Rain Attenuation Levels

Frequency (GHz)	Rain Rate (mm/hr)	Attenuation Coefficient (dB/km)	Total, Two-Way Attenuation (dB)	
			1 km Rain Cell Height	5 km Rain Cell Height
13.5	2	0.06	0.12	0.6
	10	0.4	0.8	4.0
	20	0.9	1.8	9.0
35	2	0.5	1.0	5.0
	10	2.4	4.8	24.0
	20	5	10.	50.0

Table 3 Track Point Error for Single Cloud Case (Cloud thickness = 1 km; Liquid water content = 1 gm/m^3)

Frequency (GHz)	SWH (m)	Track Point Shift (cm)		
		Maximum Instantaneous	1 Second Average	3 Second Average
13.5	2	3.9	2.2	0.6
13.5	4	8.0	4.0	1.2
35	2	17.6	6.3	2.9
35	4	41.5	20.4	7.2

1 km and 5 km rain cell height. Note that at 13.5 GHz and a 5 km rain cell height, the total attenuation varies between 0.6 and 9 dB and at 35 GHz, it varies between 5 and 50 dB over the rain rate range 2-20 mm/hr.

3. ALTIMETER PRECISION DEGRADATION

The effect of clouds and rain on altimeter performance is dependent upon two parameters: the spatial scales of attenuation variability relative to the altimeter beam-limited footprint and the magnitude of the attenuation.

In this section we will model the effect on the altimeter estimate of the range to mean sea level as it passes over (1) plausible, idealized cloud and rain attenuation patterns and (2) actually measured rain cell attenuation patterns.

3.1 Simulation of Altimeter Return Waveform Distortion

Figure 1 provides a schematic representation of the geometry of the simulations employed to estimate waveform shape distortions caused by various attenuation patterns. Each annular region in the altimeter footprint corresponds to a constant ocean surface area responsible for backscatter into a single range bin. An idealized, cylindrical attenuation cell is shown to intersect the footprint. This cell may represent either a cloud or a rain cell. It is clear that different fractions of each annular region intersect with the given cell. Hence, a different attenuation level may be associated with each range bin. Construction of the return pulse shape was performed for one annular region at a time. Each annular region was subdivided into 16 angular sections. For each one of these sections the power return to the radar was calculated assuming no fading noise present. The calculation included any attenuation. The angular sections were integrated to obtain the power from an entire annular region. This power was in turn weighted by the antenna pattern to estimate the power return in the appropriate range bin. In this way, the entire waveform shape was constructed, range-bin-by-range-bin.

The estimate of the position of the leading edge of the return pulse is dependent upon the particular tracking algorithm used. The tracking algorithm used on Seasat was chosen because its track point bias at high sea states is much lower than that of a threshold level tracking algorithm (MacArthur, 1978). The Seasat algorithm used the entire waveform shape to fashion its track point estimate. The simulations undertaken employed the Seasat tracking algorithm to determine track point position.

In these simulations we examined altimeter operating at 13.5 and 35 GHz, with a 1 m dish at an altitude of 800 km with a ground track velocity of 7 km/s.

3.2 Idealized Cloud and Rain Cell Attenuation Patterns

Three idealized rain/cloud models were chosen to demonstrate the effect of rain and cloud attenuation on the altimeter measurement of the range to mean sea level. Although these models are idealized,

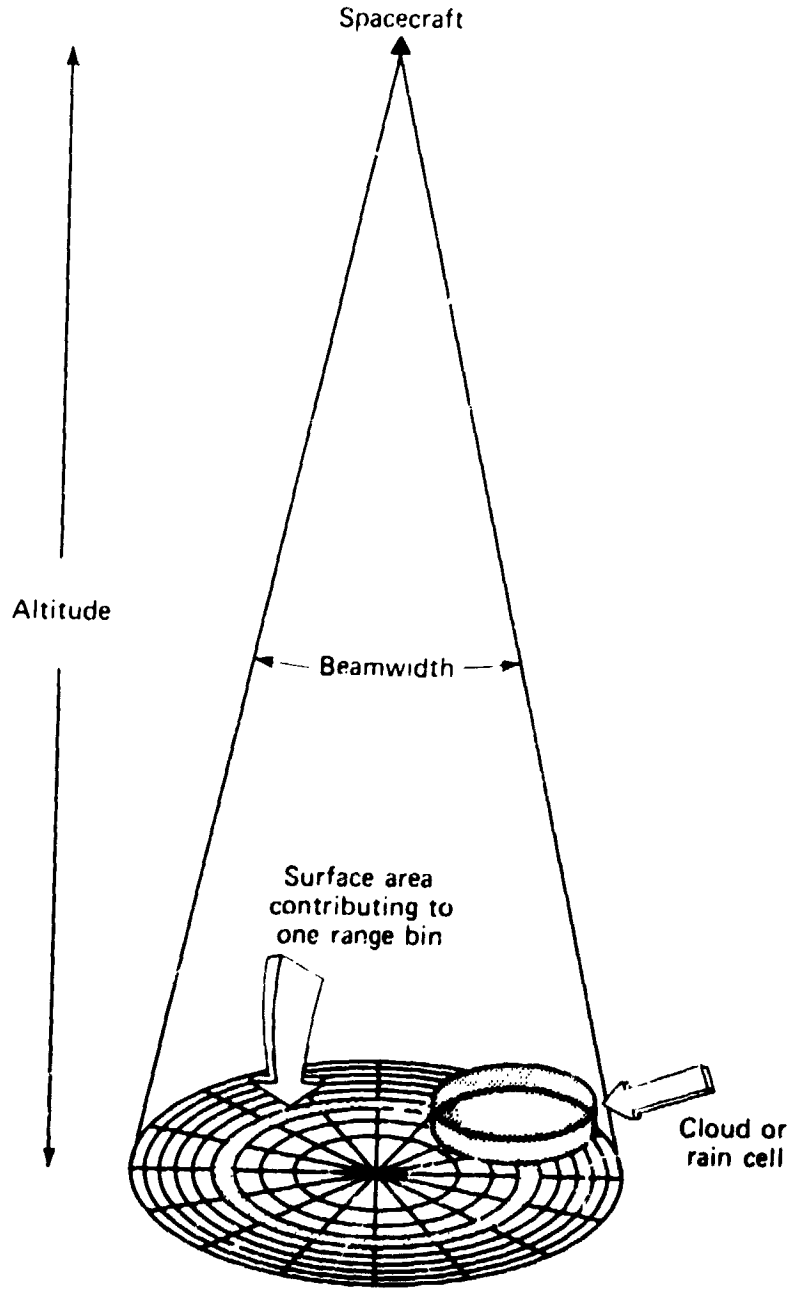

Figure 1 Altimeter-Attenuation Cell Configuration

they were chosen to represent plausible rain and cloud attenuation levels and scale sizes consistent with those discussed in Section 2.

The following rain/cloud models were considered in this analysis: (1) A cylindrical cloud of 5 km diameter and 1 km thickness with a liquid water content, M, of 1 gm/m^3. (2) A cylindrical rain cell of 5 km diameter and 5 km thickness with a rain rate of 10 mm/hr. (3) A sinusoidally attenuating cloud medium with spatial wavelengths of 5, 2.5, and 1.0 km. The maximum two-way attenuation being 0.34 dB at 13.5 GHz and 2.2 dB at 35 GHz (M=1 gm/m^3). This type of cloud variation is representative of the periodic attenuation associated with "cloud streets". For models 1 and 2 the altimeter is assumed to pass directly over the cloud or rain cell center. In model 3, the altimeter ground track is assumed perpendicular to the cloud street crests.

For the single cloud condition described above, the instantaneous track point shift can be quite significant, but when averaged over a 1 or 3 s interval, the mean track point shift reduces substantially (Table 3). For the 35 GHz case, the mean track point error is still large compared to the TOPEX requirement of a few centimeter precision (TOPEX Science Working Group Report, 1981).

Table 4 presents the track point shift associated with cloud streets. Note that as the wavelength of the cloud streets decreases, the track point shift gets smaller. This is because the attenuation variations begin to occur at small enough scales that they are partially averaged over within each pulse. The table also indicates that the maximum track point shift is much higher for 35 GHz than for 13.5 GHz.

It is also important to note that track point errors generally increase with significant wave height (SWH). At larger ocean wave heights, the return pulse is spread out smearing the leading edge of the pulse. This is further compounded by the introduction of a spatially variable attenuation described here.

Consider now track point shifts for the case of the single cylindrical rain cell of 5 km height and 10 mm/hr rain rate. It is clear from Table 5 that the larger attenuation values associated with rain introduce substantially greater track point shifts. Even after 1 and 3 s averages, the track point shifts at 13.5 GHz are well outside the precision requirements of Seasat, GEOSAT and TOPEX. At 35 GHz the situation is worse.

3.3 Effects Due to Measured Rain Cell Attenuation

To augment the results obtained for idealized rain patterns we considered a sample of rain attenuation profiles obtained by a ground based radar situated at Wallops Island, Virginia. The attenuation profile was constructed from a corresponding radar reflectivity profile employing a low elevation radar scan (Goldhirsh, 1979). The radar reflectivity corresponding to each adjacent pulse volume of resolution 150 m was converted to an equivalent attenuation coefficient employing an empirical relation derived from measured rain drop size distribution data (Goldhirsh, 1979). The integrated

Table 4 Maximum Instantaneous Track Point Shifts for the Cloud Street Case (Maximum Liquid Water Content = 1 gm/m^3)

Frequency (GHz)	SWH (m)	Track Point Shift at Various Cloud Street Wavelengths (cm)		
		1.0 km	2.5 km	5.0 km
13.5	2	0.7	0.9	2.6
35	2	6.4	8.3	13.3

Table 5 Track Point Error for Rain Cell Case (Rain Height = 5 km; Rain Rate = 10 mm/hr)

Frequency (GHz)	SWH (m)	Track Point Shift (cm)		
		Maximum Instantaneous	1 Second Average	3 Second Average
13.5	2	97.1	45.7	14.9
13.5	4	93.2	50.5	15.6
35	2	119.7	64.6	21.7
35	4	150.6	86.6	30.6

Table 6 Track Point Shifts for a Measured Rain Attenuation Case. Assumes 2 m SWH.

Frequency (GHz)	Maximum Attenuation (dB)	Track Point Shifts (cm)		
		Maximum Instant.	RMS of 1 Second Averages	RMS of 3 Second Averages
13.5	9.7	25.3	3.5	1.1
35	47.4	124.7	14.7	10.2

attenuation with height was constructed assuming the rain to be uniform with altitude over a 4 km cell height. Figure 2a shows the resulting attenuation profile associated with an estimated maximum rain rate of about 25 mm/hr. The actual attenuation at 13.5 GHz varies from 0 to 9 dB. In Figure 2b track point errors induced by this attenuation are plotted for a SWH of 2 m. A similar simulation was derived at 35 GHz (not shown).

Results of these simulations are given in Table 6. Instantaneous track point errors are many centimeters at both frequencies. By averaging over 1 to 3 seconds the track point errors at 13.5 GHz are reduced to 3.5 and 1.1 cm, respectively. At 35 CHz the instantaneous error can be many tens of centimeters and the averaged errors still exceed 10 cm. Much larger track point errors at 35 GHz as opposed 13.5 GHz are caused by both the larger attenuations at 35 GHz and the smaller footprint of the beam.

Two additional points are worthwhile noting. First, the track point shift in Figure 2b shows no mean trend as the mean absorption of Figure 2a increases. This emphasizes our earlier statement that only inhomogeneities of absorption cause track point shifts. Second, the results of Table 6 for 35 GHz are somewhat academic because no actual radar would have sufficient signal-to-noise margin to be able to tolerate a 47 dB attenuation and maintain track.

4. CONCLUSIONS

We have demonstrated for both idealized rain and cloud configurations as well as measured rain rate variabilities, significant altimeter degradation may occur at 13.5 and 35 GHz. Although averaging track points over several seconds may mitigate these errors, they may still be unacceptably high.

At 13.5 GHz, the effect of clouds on the average track point shift is generally small (approximately 1 cm for cylindrical model and less than 3 cm for the cloud street model). On the other hand, rain rates as high as 10 mm/hr may produce unacceptably high range uncertainties (e.g., isolated rain cell case).

At 35 GHz, both the effects of clouds and rain may, in general, seriously degrade the track point errors. Errors as high as 7 cm for isolated clouds and 13 cm for cloud streets may occur. For rain rates of 10 mm/hr, absorptions as high as 47 dB and track point errors as high as 31 cm may be produced. The employment of future conventional type altimeter systems operating at 35 GHz and higher is not recommended.

Since track point errors at 13.5 GHz may seriously be degraded by rain, it is recommended that future altimeters operating at this frequency employ rain detecting capabilities to flag rain corrupted data.

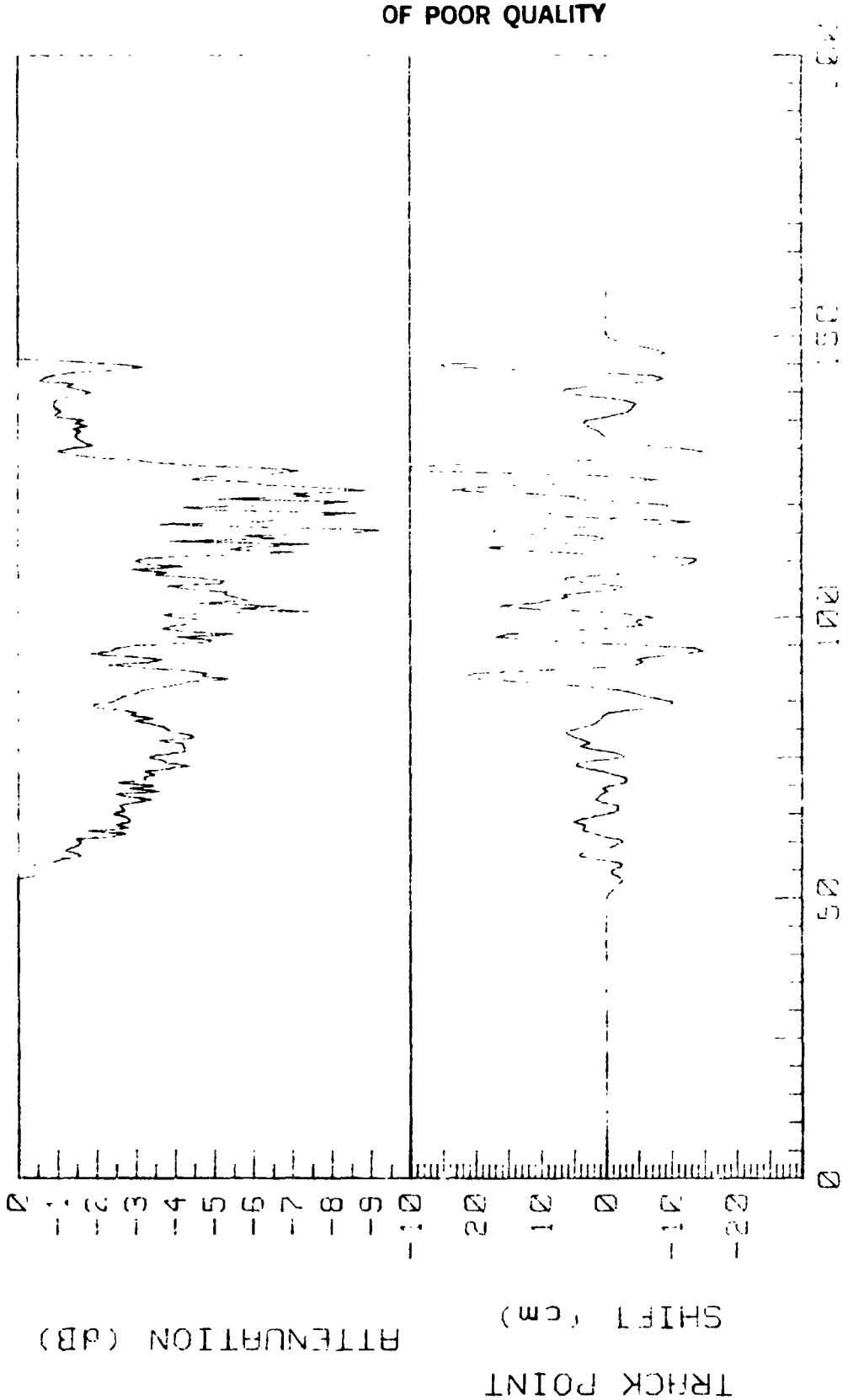

Figure 2 Track Point Shift and Measured Attenuation at 13.5 GHz as a Function of Ground Track Position

5. REFERENCES

Ackerman, B., 1959, "The Variability of the Water Contents of Tropical Cumuli", J. of Appl. Meteorology, Vol. 16, April, pp. 191-198.

Ackerman, B., 1967, "The Nature of Meteorological Fluctuations in Clouds", J. of Appl. Meteorology, Vol. 6, February, pp. 61-71.

Cole, A.E., 1961, "Handbook of Geophysics", (Chapter 7, Clouds), The Macmillan Company, New York, p. 88.

Goldhirsh, J., 1979, "A Review on the Application of Non-attenuating Frequency Radars for Estimating Rain Attenuation and Space Diversity Performance", IEEE Transactions on Geoscience Electronics, Vol. GE-17, No. 4, October, pp. 218-239.

Goldhirsh, J. and J.R. Rowland, 1982, "A Tutorial Assessment of Atmospheric Height Uncertainties for High Precision Satellite Altimeter Missions to Monitor Ocean Currents", IEEE Trans. on Geosci. and Remote Sensing, Vol. GE-20, No. 4, October, pp. 418-434.

Gunn, K.L.S. and T.W.R. East, 1954, "The Microwave Properties of Precipitation Particles", Q. J. of the Royal Meteor. Soc., Vol. 80, pp. 522-545.

Kuettner, J.P., 1971, "Cloud Bands in the Earth's Atmosphere - Observation and Theory", Tellus, Vol. 23, pp. 404-425.

Lopez, R.F., 1977, "The Lognormal Distribution and Cumulus Cloud Populations", Monthly Weather Review, Vol. 105, July, pp. 865-872.

MacArthur, J.L., 1978, "Seasat-A Radar Altimeter Design Description", JHU/APL Technical Report SDO-5232, November.

Marshall, J.S. and W. McK. Palmer, 1948, "The Distribution of Rain Drops with Size", J. Meteorology, Vol. 5, pp. 165-166.

TOPEX Science Working Group Report, 1981, "Satellite Altimetric Measurement of the Ocean", Jet Propulsion Laboratory, Pasadena, CA., Tech. Rep. Document No. 400-111, March.

Walsh, E., F.M. Monaldo and J. Goldhirsh, "Rain and Cloud Effects on a Satellite Dual Frequency Radar Altimeter Operating at 13.5 and 35 GHz", IEEE Trans. on Geosci. and Remote Sensing, in press.